ChemComm

HIGHLIGHT

View Article Online
View Journal | View Issue

Cite this: *Chem. Commun.*, 2025, **61**, 2190

Dynamic restructuring of electrocatalysts in the activation of small molecules: challenges and opportunities

Hsiwen Wu[a] and Jie Zhang *[abc]

Received 1st October 2024,
Accepted 30th December 2024

DOI: 10.1039/d4cc05165c

rsc.li/chemcomm

Electrochemical activation of small molecules plays an essential role in sustainable electrosynthesis, environmental technologies, energy storage and conversion. The dynamic structural changes of catalysts during the course of electrochemical reactions pose challenges in the study of reaction kinetics and the design of potent catalysts. This short review aims to provide a balanced view of *in situ* restructuring of electrocatalysts, including its fundamental thermodynamic origins and how these compare to those in thermal and photocatalysis, and highlighting both the positive and negative impacts of *in situ* restructuring on the electrocatalyst performance. To this end, examples of *in situ* electrocatalyst restructuring within a focused scope of reactions (*i.e.* electrochemical CO_2 reduction, hydrogen evolution, oxygen reduction and evolution, and dinitrogen and nitrate reduction) are used to demonstrate how restructuring can benefit or adversely affect the desired process outcome. Prospects of manipulating *in situ* restructuring towards an energy-efficient and durable electrocatalytic process are discussed. The practicality of pulse electrolysis on an industrial scale is questioned, and the need for genius schemes, such as self-healing catalysis, is emphasized.

1. Introduction

Stable performance of catalyst (*i.e.* maintaining its activity and selectivity over an extended duration) is a key consideration in chemical processes. In heterogeneous catalysis, the interaction between catalyst surface and adsorbed species (*e.g.* reactants, intermediates, products, *etc.*) and that with the surroundings

[a] *School of Chemistry, Monash University, Clayton, VIC 3800, Australia*
[b] *ARC Research Hub for Carbon Utilisation and Recycling, Monash University, Clayton, VIC 3800, Australia*
[c] *ARC Centre of Excellence for Green Electrochemical Transformation of Carbon Dioxide, Monash University, Clayton, VIC 3800, Australia.*
E-mail: jie.zhang@monash.edu

Hsiwen Wu

Hsiwen Wu obtained his PhD (2021) in Chemical and Biomolecular Engineering at the Hong Kong University of Science and Technology. He is now a research fellow at the Monash University School of Chemistry. His research interests include the electrochemical reduction of CO_2, electrocatalysts for oxygen reduction reactions, hydrogen fuel cells, and membrane electrode assembly design.

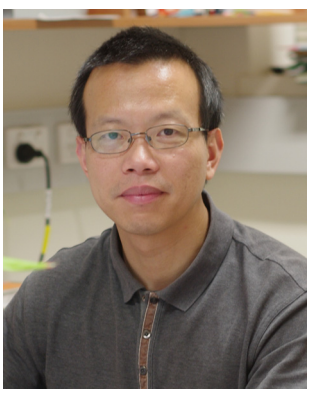

Jie Zhang

Jie Zhang is an Associate Professor at the School of Chemistry, Monash University, and a Chief Investigator, Research Program Leader and co-Theme Leader for the Australian Research Council (ARC) Centre of Excellence for Green Electrochemical Transformation of Carbon Dioxide and the ARC Research Hub for Carbon Utilisation and Recycling. His current research mainly focuses on the electrochemical activation of small molecules for energy and sensing and the development and applications of artificial intelligence in dynamic electrochemistry.

(*e.g.* temperature, applied electric potential, radiation, *etc.*) often induce structural transformation of the catalyst during reaction. Such restructuring can be morphological and/or compositional, and the spatial and temporal scales of which can span from nano- to micrometers, and from sub-seconds to hours, respectively.[1] Based on the energy input/output, heterogeneous catalysis can be categorized into thermal-, electro-, and photocatalysis, and the catalyst restructuring involved in each is highly related to the energetics near the catalyst surface.[2] In thermal catalysis, energy is supplied to the catalyst as heat to produce phonons, and the change in reaction Gibbs free energy from varying reaction conditions is usually less than several tens of milli-eV. Given that reaction enthalpy is a weak function of temperature, a change in temperature by 100 °C for example only results in milli-eV level difference in reaction Gibbs free energy (the exact value depends on the molar entropy change of the reaction of interest). In electro- and photocatalysis, the Gibbs free energy involved is notably larger (*e.g.* an applied/output voltage of several volts is common in electrocatalysis; while photoexcitation at around 3 eV is frequently seen in semiconductors to generate charge separation in photocatalysis[3,4]) and therefore is accompanied by pronounced structural change and often deactivation. In addition, the flow of electrons across multiple interfaces is involved in electrocatalysis (*i.e.* electrolyte/catalyst, catalyst/support, support/current collector, *etc.*) and in photocatalysis (*i.e.* metal/dielectric support, *etc.*), where the accumulation charge tends to occur at locations of high surface curvature. Such inhomogeneity in surface charge distribution may produce extremely high local current density[5] and lead to catalyst restructuring and/or corrosion of other components.[6]

It should be noted that the restructuring of catalyst is dynamic throughout the course of reaction and that the freshly prepared catalyst functions only as a pre-catalyst, as the active sites of the former are most likely different from those during operating reaction conditions.[1,2] Based on the above, promotors are often incorporated into pre-catalysts to guide the structural transformation towards enhanced catalytic performance[7] (*i.e.* mass/volume normalized turnover frequency, selectivity towards the target product, and durability). In the Haber–Bosch process, for example, structural promoters such as Al_2O_3 and CaO are incorporated into iron oxides to stabilize the grain boundaries of the latter against sintering.[8,9] Potassium oxide is used as an electronic promoter in the Haber–Bosch process, which in its active form facilitates the dissociative adsorption of dinitrogen.[10] As another example, in electrochemical CO_2 reduction (ECO_2R), halide ions in the electrolyte[11–16] are used as promoters to steer the restructuring of copper oxides[17–22]/halides[23] towards a roughened Cu surface under applied potentials, which results in improved selectivity to multi-carbon products.[24–26]

While comprehensive reviews focusing on the *in situ* restructuring of electrocatalysts in one specific reaction (*e.g.* ECO_2R,[27] OER,[28–32] *etc.*) or on characterization techniques that track the species and structural evolution during electrocatalytic reactions[33,34] are available, works covering the fundamental driving force of restructuring in electrocatalysis over a range of reactions[35–38] and how it compares with other heterogeneous catalytic reactions (*i.e.* thermal and photocatalysis)[2] are relatively few. In this short review, a balanced view of electrocatalyst reconstruction is provided, including its thermodynamic origins and the associated positive and negative effects on catalytic performance. While the aim is not to cover all electrocatalytic reactions involving simple molecules, we focus on the *in situ* restructuring of electrocatalysts during the activation of small molecules (*e.g.* CO_2, H_2, O_2, N_2 and NO_3^-) as examples to demonstrate the general applicability of the thermodynamic driving force and highlight the possibility of achieving enhanced catalytic performance through controlled restructuring. The thermodynamic origins of restructuring in electrocatalysis are first introduced and collated with those in thermal and photocatalysis. Next, examples of how *in situ* restructuring adversely impacts the electrocatalytic performance are presented, followed by the opposite cases where it benefits the outcome of electrocatalysis. Finally, perspectives and outlooks on regulated restructuring towards energy-efficient and durable electrocatalytic processes are presented.

2. Origins of restructuring in electrocatalysis

The restructuring of electrocatalysts occurs under reaction conditions to decrease the net free energy of the system. The fact that the state of the electrocatalytic system changes during cell operation (*e.g.* change in electrode potential, species concentration, exposed surface area, *etc.*) suggests that the driving force for catalyst restructuring also varies throughout the reaction. Origins leading to such dynamic restructuring can be classified into three categories: surface energy reduction, electrode potential, and interaction with an electrolyte and adsorbed species. The following describes how each serves as the driving force for *in situ* structural transformation.

2.1. Surface energy reduction

In a system of particles, the thermodynamic tendency is to lower the energy of the system through the reduction of the surface free energy. This driving force is fundamental and universal, and the effects of which can be observed throughout heterogeneous catalysis (*i.e.* electro-, thermal-, and photocatalysis). Phenomena associated with surface energy reduction include aggregation (assembly of particles with individual boundary maintained),[39] coalescence (merge of particles in which individual boundary is lost),[40] sintering (merge of particles when the temperature is elevated),[41] and Ostwald ripening (dissolution of high-surface-energy sites followed by redeposition onto low-surface-energy sites).[40,42,43] Since surface energy reduction often results in a decreased catalytically active interface area, it is often considered as a deactivation mode in literature.[44–46] To keep a focused theme of this work on the restructuring of electrocatalysts, driving forces that are more relevant to electrocatalysis are discussed in detail in the following text.

2.2. Electrode potential

An electrocatalytic reaction involves the transfer of electrons between catalysts and reactants on an electrified surface, and

the rate of which therefore depends on the energy of electrons, which is expressed as electrode potential and carries the unit of volt (or eV, as energy carried per electron). Reaction Gibbs free energy per unit charge represents the minimal voltage required to run an electrolytic cell or the maximal voltage a galvanic cell can deliver. The activation energy barrier of an electrode reaction manifests itself as overpotential, and it outlines the importance of electrocatalysts in the energy efficiency of the catalyzed reaction. Depending on the electrode reaction (*i.e.* half-cell reaction) of interest, the operating potential window may overlap with the potential range where the catalyst is redox active, and consequently induce changes in the oxidation state of the catalyst. Cycles of oxidation and reduction of catalysts often result in the dissolution of metal constituents, and the ensuing structural change (*e.g. via* Ostwald ripening) may alter the catalyst performance significantly. For example, the OER holds a high standard reduction potential of 1.23 V *vs.* standard hydrogen electrode, under which almost all metal catalysts become oxidized and are prone to dissolution in acidic electrolytes.[31,47] As another example, in oxygen reduction reaction (ORR) in acidic media, leaching of the less noble metal in platinum alloy catalysts (PtM, M = Co,[48] Ni,[49,50] Cu,[51] Se,[52] *etc.*) is commonly reported, and the resulting dealloyed catalysts may evolve into a smooth Pt-skin or roughened Pt-skeleton structure, depending on the initial near surface composition, (Fig. 1).[53] Through *in situ* electrochemical leaching, PtM catalysts may also transform into solid or porous particles with Pt-rich shell and alloy core, depending on the initial particle size[54,55] and electrode potential.[56]

Electrode reactions operating at strongly negative (*i.e.* highly reducing) potentials can also undergo restructuring resulting from the change of oxidation state(s) in electrocatalyst component(s),[11,20,36,58,59] and/or due to cations present in the electrolyte.[60] The latter process is termed cathodic corrosion,[61,62] where cycles of cation intercalation and stripping/hydrogen evolution pulverize the crystal domain of catalysts and result in exposed high-index crystal facets.[60] An exemplary case is the instability of palladium nanocrystals in acidic electrolytes, which limits its use in hydrogen evolution reaction (HER) despite its outstanding catalytic activity.[63,64] The crystal structure of Pd allows facile incorporation of adsorbed hydrogen atoms into the lattice,[65] a phenomenon termed H absorption, and the subsequent hydrogen gas evolution at more negative potential tends to break the crystal into smaller sizes.[60] The above explains, at least partially, why restructuring of electrocatalysts is accelerated by applied electrode potential.

2.3. Interaction with the electrolyte and adsorbed species

The interaction of metal catalysts with species present in the electrolyte can lead to a considerable lowering of the reduction potential of the metal, making the dissolution of which more thermodynamically favourable. In copper-catalyzed ECO_2R for example, some of the reaction products (*i.e.* adsorbed CO and oxalate) can form stable complexes with cuprous ions and promote dissolution-related surface reconstruction, such as Ostwald ripening.[43,66] Studies on gas–solid interfaces have shown that specific adsorption (*e.g.* CO on Cu) lowers the formation energy of adatoms, especially on step edges and kinks.[67–71] Such

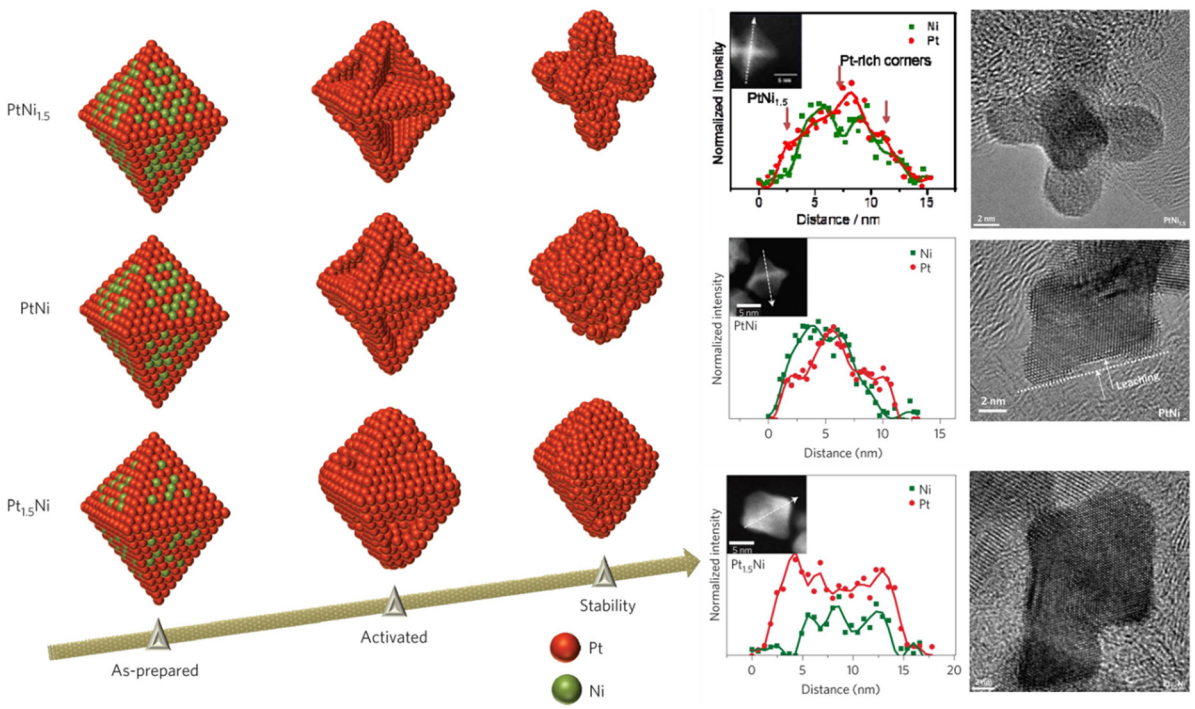

Fig. 1 Composition-dependent structural evolution of PtNi octahedra under potential cycling in an O_2-saturated 0.1 M $HClO_4$ electrolyte. As-prepared: after 3 potential cycles (0.06–1.0 V, 100 mV s^{-1}); Activated: after 25 potential cycles (0.06–1.0 V, 100 mV s^{-1}); Stability: after 4000 potential cycles (0.6–1.0 V, 50 mV s^{-1}). Figures adapted with permission from ref. 57. Copyright 2013. Springer Nature.

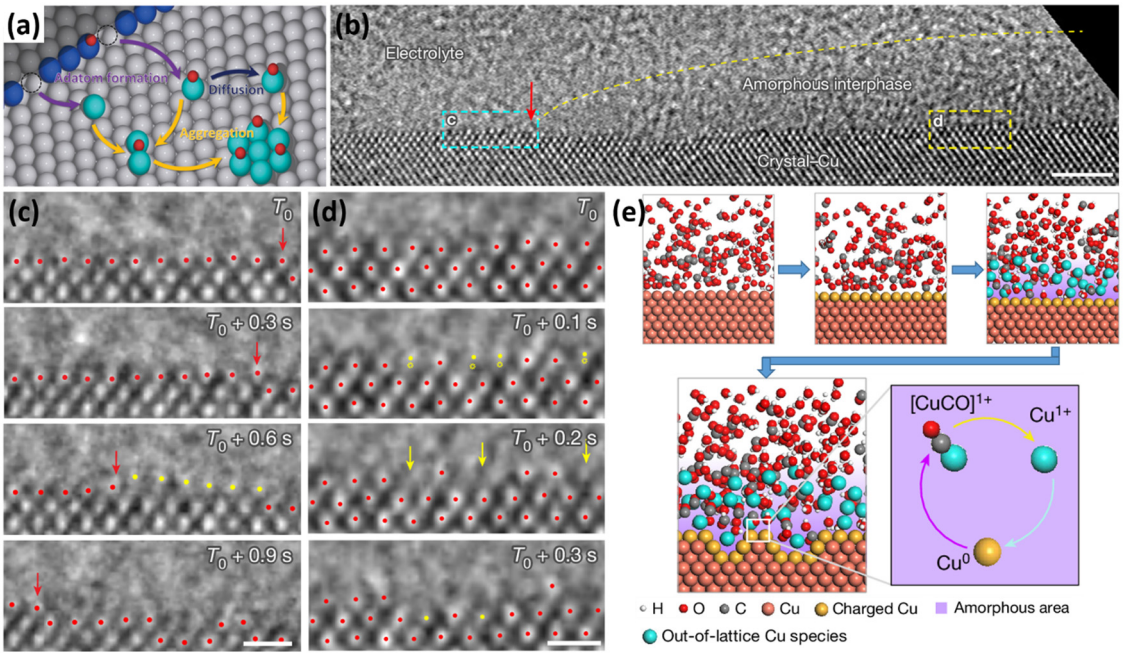

Fig. 2 Adsorbate-mediated surface reconstruction. (a) Schematic of adsorbate-decorated adatom formation, diffusion and migration on the catalyst particle surface. (b) *In situ* liquid-cell TEM image showing the amorphous interphase between the electrolyte and crystalline Cu. Scale bar, 2 nm. (c) and (d) Time-resolved magnified TEM images of regions highlighted in (b). Yellow dots and arrows signify the disappearance of Cu atoms from the crystalline phase. Scale bar 5 Å. (e) Schematic illustration of the restructuring process at the amorphous interphase. Figures adapted with permission from ref. 67 ((a)). Copyright 2023. American Association for the Advancement of Science; and ref. 82 ((b)–(e)). Copyright 2024. Springer Nature.

adsorbate-decorated adatoms have notably increased surface mobility, and tend to form nanoclusters (Fig. 2a) which function as highly active sites for thermo-catalytic reactions such CO oxidation and water–gas shift,[67,68,72,73] methanol synthesis,[69,74] ammonia synthesis/oxidation,[75,76] and Fischer–Tropsch synthesis.[76] In electrocatalytic reactions, adsorbate-promoted atom mobility on the catalyst surface is also observed in HER[77,78] and ECO_2R,[79–81] as evidenced by the *in situ* formation of undercoordinated sites similar to those reported in thermos-catalytic studies. Direct observation of adsorbate-induced highly mobile Cu surface has been achieved *via in situ* liquid-cell transmission electron microscopy (TEM), and the former is visualized as an amorphous fluid-like layer flowing across the crystalline Cu surface (Fig. 2b–e).[82] For metal alloy catalysts, the interaction with species present in the electrolyte may lead to segregation, the separation of the originally uniform phase into multiple domains of different compositions. For example, CuAg alloy catalyst during ECO_2R may phase-separate into a core–shell structure with a Cu-rich surface[80,83] due to stronger binding energy of CO on Cu than that on Ag.[84]

In many instances, the effects of the electrode potential and adsorbate/electrolyte species are intertwined, and both contribute to the restructuring of catalysts. In ECO_2R, the reversible generation/disappearance of Cu nanoclusters from nitrogen-coordinated Cu single-atom catalysts with respect to applied potential has been observed *via in situ* X-ray absorption spectroscopy (XAS).[85–87] While the formation of clusters from single-atom sites is induced by adsorbate-promoted mobility (*i.e.* *H–Cu[88] and CO–Cu[89]) under applied potential, the redispersion of clusters back to nitrogen-coordinated single-atoms is facilitated by hydroxyl radicals produced from the reaction between water molecules and bicarbonate anions near cathode at open-circuit potential.[88,90] In OER, the strongly oxidizing electrode potential transforms metal nanoparticle pre-catalyst into oxides, and the lattice oxygen mechanism suggests that oxygen atoms in the metal oxide crystal are constantly ejected as O_2 gas, and replenished from adsorbed hydroxide anions.[91–96] In this case, the effects of adsorbed hydroxide and electrode potential on OER catalyst restructuring are intertwined and both contribute to the lattice oxygen mechanism.

3. Impacts of *in situ* catalyst restructuring on electrocatalytic performance

In the previous section, we see that the restructuring of electrocatalysts depends on multiple (coupled) factors and that the structural change of the catalyst is dynamic throughout the course of the reaction. The impact of restructuring can be beneficial or unfavourable to the catalyzed process, depending on the targeted outcome. The following text discusses the negative and positive impacts of *in situ* catalyst restructuring, using reports on ORR, OER, ECO_2R, HER, and nitrogen electro-redox reactions as examples.

3.1. Negative impacts

In situ restructuring of electrocatalysts often results in diminished activity and/or selectivity on an industrially-relevant time

scale, if not on a laboratory time scale. Therefore, control strategies towards mitigated or regulated restructuring are at the focal point of electrocatalysis research. In the following, cases where restructured electrocatalysts deliver decreased activity and/or selectivity are discussed.

Electrocatalysts operating under high electrode potentials (*e.g.* OER and ORR catalysts) are prone to metal dissolution. In general, leaching of metal in the cell may lead to deactivation in two folds. One is the loss of electronic and geometric effects beneficial to the activity enhancement, and the other relates to the adverse effects of leached metals on other cell components (*i.e.* deposition on a low-potential electrode,[97] deposition within the membrane electrolyte,[98,99] Fenton reaction that promotes membrane degradation,[100] *etc.*). In PtM (M is a less noble metal than Pt) ORR catalysts, the outcome of *in situ* restructuring depends on the interplay of M dissolution and Pt surface diffusion,[55] and is strongly potential dependent, as evidenced by several *in situ* characterization techniques on PtNi ORR catalyst.[56] At the normal operating potential range of proton exchange membrane fuel cell (PEMFC) cathode, 0.6–1.0 V *vs.* reversible hydrogen electrode (RHE), PtNi particles maintain their structure (probed *via in situ* electrochemical atomic force microscopy) despite pronounced leaching of Ni content, as verified *via* on-line inductively coupled plasma mass spectrometry. However, at extremely high potentials of 1.3–1.5 V *vs.* RHE, which occur transiently during the start-up and shut down of the PEMFC, significant coalescence was observed as the *in situ* grazing-incidence small-angle X-ray scattering data suggested a notably increased particle diameter, standard deviation of the particle diameter, and minimum interparticle distance, while the volume fraction of Pt nanoparticles decreases.[56] Upon metal leaching, the ensuing change in the catalyst particle size (*i.e.* wider particle size distribution) and the roughened surface with high-surface-energy sites exposed favour Ostwald ripening.[101] The effects of leaching are observed in PEMFC cathode as increased catalyst particle size for Pt and PtM (M = Co, Ni) catalysts,[102,103] as hollow Pt shells for Pt@Pd core–shell catalysts,[104] as the appearance of a Pt-[98,105] or Pd-band[99] in the membrane.

Segregation is a common issue in electrocatalysis, where the near-surface composition of a synthesized pre-catalyst is altered *via* nanoscale rearrangement of constituent atoms into different phases under electrochemical conditions. Aside from electrode potential and possible adsorbate that change dynamically during the reaction, the influence of ambient oxygen on catalyst segregation can be a critical factor for the stability of alloy catalysts according to density functional theory (DFT) calculations, and therefore should also be included as a design consideration.[106] While catalyst segregation can be readily regulated in thermal catalysis through activation or regeneration under a selected reducing atmosphere,[107–112] reliable control of segregation in electrocatalysis can be challenging due partly to the increased system complexity.[106] When aiming to direct an electrocatalyst towards targeted phase(s) (*e.g.* solid-solution, intermetallic, core–shell, *etc.*) through the applied potential for example, factors such as the electrolyte pH, possible adsorbates, and the electrochemical window of the solvent are coupled to the electrode potential and impact the outcome of segregation. In ECO_2R, segregation usually deactivates alloy catalysts through the removal of sites for C–C coupling,[113] loss of targeted electronic interaction,[80,114] or coverage of ECO_2R-inactive metal on the surface.[115] For example, X-ray absorption fine-structure spectroscopy (XAFS) was used to track the evolution of oxidation state and coordination environment of constituents in CuZn catalyst during ECO_2R, and it was discovered that phase-segregated Cu–ZnO promotes methane production, while solid solution CuZn formed after prolonged operation suffers from pronounced HER.[114] As another example, through *in situ* nuclear resonant inelastic X-ray scattering and XAFS, it was observed that iron atoms in CuFe alloy segregate to the surface during ECO_2R due to the stronger adsorption energy to CO intermediate, resulting in an enhanced HER.[115]

The restructuring of the catalyst in ECO_2R is specific with respect to the product–metal pair, and the combined effects of multiple processes eventually lead to deactivation of the catalyst.[44–46] In Cu-catalyzed ECO_2R for example, the reaction intermediate/product of *CO (adsorbed intermediate) and oxalate can interact strongly with Cu, and stabilize cuprous (Cu^+) cation in the solution phase, therefore exacerbating dissolution-related structural transformation.[43,66,116] The structural evolution of Cu nanoparticles in ECO_2R generally follows a chronological order of cathodic corrosion, aggregation and coalescence, surface roughening and smoothening, resulting from dissolution–deposition, adatom migration, *etc.*[117] Some of these processes are captured nicely using *in situ* liquid-cell TEM, such as cathodic corrosion,[117–119] adsorbate-induced atomic migration[82] and segregation,[80] Ostwald ripening[43] and coalescence (Fig. 3).[117] Cu-based catalysts may initially experience a period of activation (*i.e.* increasing selectivity for multicarbon products with respect to time) due to the exposure of high-index crystal facets from cathodic corrosion and adsorbate-induced formation of nanoclusters. At a time scale relevant to industrial applications, however, the activity towards the target product decreases as Ostwald ripening and coalescence gradually take effects, as shown in Fig. 3.[117]

In electrochemical ammonia synthesis from dinitrogen[120,121] or nitrate,[122–125] HER is a major side-reaction similar to the case of ECO_2R. *In situ* restructuring during ammonia synthesis may lead to increased selectivity towards HER, especially under highly cathodic overpotentials.[123,126] Manipulation of the morphology of pre-catalyst has been shown to enhance the electrochemical dinitrogen reduction reaction (e-NRR) through suppressing HER[127,128] and enhanced adsorption of dinitrogen on the catalyst surface.[129] It should be noted that the identification of restructuring during e-NRR can be quite challenging, as the background/artefact of the dominant HER often masks the structural evolution due solely to e-NRR.[130] In electrochemical dinitrogen oxidation reaction (N_2OR) to nitrate, activation of dinitrogen and suppression of parasitic OER are the two major challenges in catalyst design.[131] In this case, *in situ* restructuring of N_2OR catalyst towards a defect-rich oxide/oxyhydroxide is undesirable,[132–134] as such amorphous layers favor OER.[135] For example, in N_2OR *via* oxygen-vacancy-enriched tin oxide, enhanced faradaic efficiency

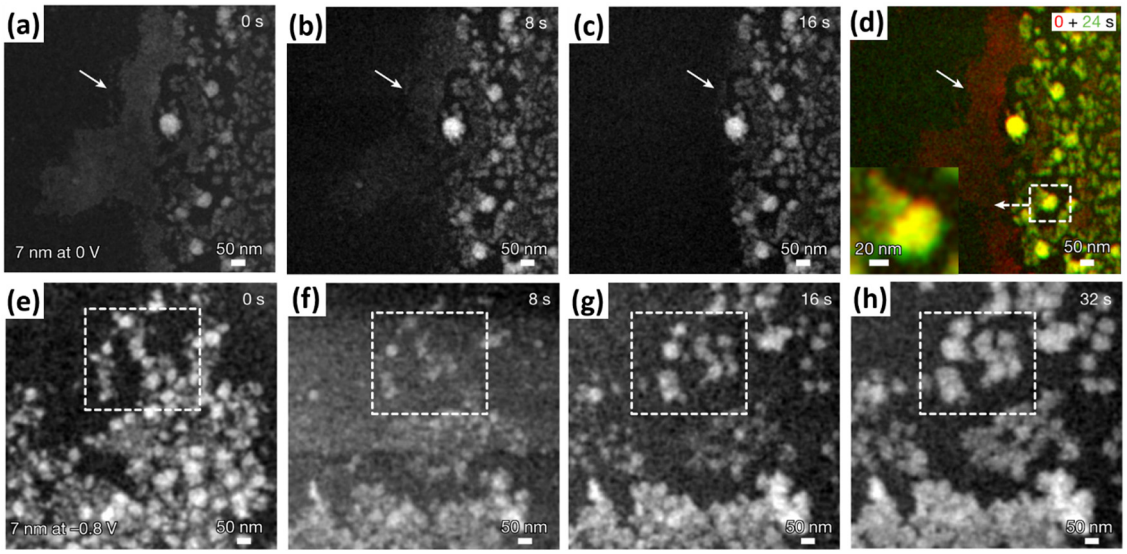

Fig. 3 *In situ* liquid-cell TEM images capturing the time evolution of Cu nanoparticles at different electrode potentials. (a)–(d) at open-circuit potential at time = 0, 8, 16, and 24 seconds. (e)–(h) under −0.8 V *vs.* RHE at time = 0, 8, 16, and 32 seconds. Figures adapted with permission from ref. 117. Copyright 2023. Springer Nature.

and yield towards nitrate were attributed to decreased activation energy barrier for the activation of $*N_2$ to $*N_2OH$ through DFT calculations.[134]

Aggregation and coalescence are mechanisms that apply to a system of particles, irrespective of the specific electrochemical reaction. Coalescence usually follows aggregation as the former further reduces the surface energy of the system by eliminating the surface area of the interface, and both lead to a decrease in the number of accessible active sites.[136] Exemplary cases of proper anchoring of molecular catalyst (*e.g.* cobalt phthalocyanine) on the selected substrate (*e.g.* functionalized carbon nanotube, graphene) against aggregation and coalescence have been demonstrated in ORR[137,138] and ECO_2R,[139–143] where the electronic interaction not only immobilize the catalyst molecule, but also fine-tune its catalytic property. Immobilization of single atom active sites into an extended network (*i.e.* metal–organic frameworks,[139,144] covalent organic frameworks[145]) contributes to increased site density,[142,143,146,147] but the stability of these frameworks under electrochemical conditions (*i.e.* combined effects of the applied electrode potential and electrolyte pH) remains a challenge for long-term operation.[148,149] For nanoparticle catalysts, physical confinement through carbon-based support has found some success in delaying the aggregation in the HER,[150] OER,[151] ORR[152,153] and ECO_2R.[154–156]

3.2. Positive impacts

In instances where the active form generated from pre-catalyst demonstrates favoured catalytic performance (such as improved selectivity towards a specific product, enhanced reaction kinetics, *etc.*) but is rather short-lived, approaches to induce restructuring that leads to the regeneration of desired active form are often implemented. Stabilization of the active form may also be achieved through the design of pre-catalyst and/or pre-treatment methods prior to cell operation. In the following, instances where electrocatalytic activity and/or selectivity are improved through restructuring are analyzed.

Regulated metal leaching can be used to prepare stable ORR catalysts prior to PEMFC assembly. Potential cycling of PtM alloy catalyst in a selected acidic electrolyte followed by thermal annealing has been shown to produce core–shell structure with a Pt-rich shell (often termed the Pt-skin catalyst) stable against metal leaching under PEMFC relevant conditions.[53,57,157] For Pt@Pd catalysts, controlled Pd-leaching in the presence of a capping agent allows the rearrangement of Pt atoms in the shell, which is proposed to repair the pinhole defects. The treated Pt@Pd catalyst shows a Pt shell with increased thickness, and in PEMFC tests demonstrates notably improved durability, which is supported by the significantly lowered Pd dissolution rate.[104] Non-precious metal ORR catalysts are promising alternatives to state-of-the-art Pt-based catalysts when operating under neutral or alkaline conditions.[158,159] Metal leaching is also common in non-precious metal catalysts during ORR, and through rational pre-catalyst design (*i.e.* pairing of a metal cation and a p-block anion), a metastable amorphous layer with enhanced ORR activity can be generated *via in situ* restructuring.[160,161] The above metal-leaching-induced restructuring of ORR catalysts was mostly studied in rotating disk electrode experiments, and caution should be given that the observed activity enhancement overlooks the possibility of ionomer/membrane poisoning in practical fuel cell test setup.

In HER, catalysts with abundant basal plane active sites have been shown to demonstrate "self-optimizing behaviour", where stacked catalyst layers become exfoliated and expose more active sites during the course of HER (Fig. 4a–c).[162] Similar to the amorphous surface layer formed through leaching of ORR catalyst component(s) introduced earlier, proper design of HER pre-catalyst leads to a metastable and highly active phase that benefits the electrocatalytic process.[135,163] For example, vanadium-doped

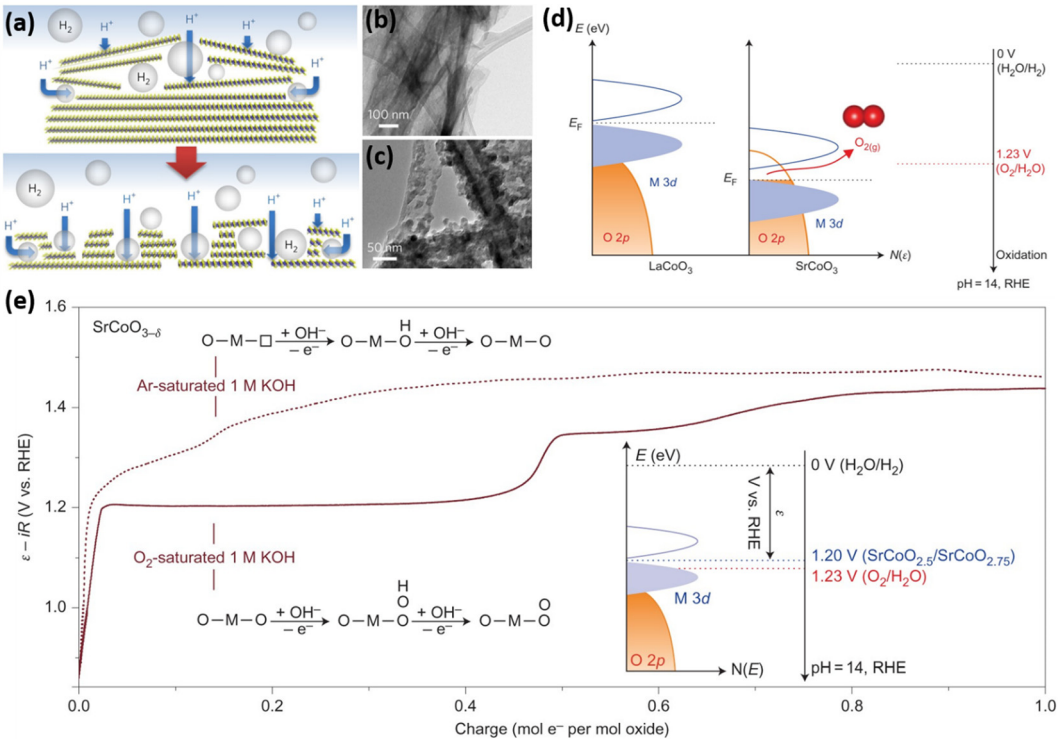

Fig. 4 *In situ* restructuring of electrocatalysts that lead to beneficial catalytic performance. (a) schematic illustration of the "self-optimizing behaviour" of layered TaS_2 catalysts. (b), (c) TEM images of TaS_2 before, and after HER potential cycling. (d) Schematic band diagrams of perovskite oxide $LaCoO_3$ and $SrCoO_3$, compared to the redox energy of the O_2/H_2O couple. (e) Galvanostatic charging of $SrCoO_{3-\delta}$, an oxygen-vacancy-rich oxide, in an O_2- and Ar-saturated alkaline electrolyte, demonstrating the effectiveness of the lattice oxygen mechanism in lowering the reaction overpotential. Figures adapted with permission from ref. 162 ((a)–(c)). Copyright 2017. Springer Nature; and ref. 168 ((d) and (e)). Copyright 2017. Springer Nature.

nickel sulfide is restructured to form an amorphous surface layer, which demonstrates superior HER activity relative to the control without V-doping.[163] Defect engineering through the incorporation of an easily leachable component in the pre-catalyst is another way to facilitate regulated restructuring.[164] In ECO_2R, the stronger binding energy of *CO on defect-rich Cu sites relative to that on low-index Cu crystal facets has been shown to favour the selectivity towards multi-carbon products, through increased surface coverage of *CO and decreased energy barrier for C–C coupling.[24,165] The use of Cu oxides[11,18–22,24–26] or chlorides[23] as pre-catalysts facilitates the generation of undercoordinated sites upon *in situ* reduction of Cu under ECO_2R relevant potentials. The rational use of ligand promotes the *in situ* selective faceting of Cu nanocrystals under ECO_2R conditions, and therefore increases the faradaic efficiency towards the targeted product.[166,167]

In a bottom-up manner, pre-catalysts consisting of atomically dispersed Cu can be directed to form reversibly nanoclusters[85–88] or irreversibly nanoparticles[169] based on the applied electrode potential and achieve enhanced selectivity towards multi-carbon products. It should be noted that *in situ* generated high-index defects are high-surface-energy sites and that these sites tend to degrade over time *via* modes such as (adsorbate-induced) migration, dissolution, and coalescence.[44] Pulse electrolysis has been recognised as an effective approach to enhanced selectivity towards multi-carbon products in ECO_2R.[116,170–172] By periodically bringing the electrode potential to a less negative or even positive value, undercoordinated sites are regenerated and therefore prolong the service life of the catalyst. It should be noted that the use of pulse electrolysis to generate high-index catalyst surfaces works effectively for metals with low cohesive energy (*e.g.* Cu,[116,170–173] Ag,[171] and Bi[174]) because of the high surface atom mobility on these surfaces.[67,175] The cohesive energy of a metal is the energy required to separate atoms in the crystal into free neutral atoms in vacuum (*i.e.* metal gas),[175,176] and it serves as an indicator regarding the resistance of the metal against mobility-related structural change (*e.g.* adsorbate-induced adatom formation).[76,81,177,178] *In situ* generated high-index sites are not thermodynamically favoured, and at a longer time scale, despite the application of periodic potential pulse, the mobile metal atoms tend to migrate towards low-ohmic-resistance sites (*e.g.* contact planes between gas diffusion electrode and current collector)[179] and other low-energy sites to stabilize the system.[44]

The involvement of lattice oxygen in OER on Co-based perovskite has been confirmed *via in situ* ^{18}O isotope labelling mass spectrometry,[168] and it is expected that increasing the covalency of metal–oxygen bond makes the oxidation of lattice oxygen more thermodynamically favourable.[168] On a theoretical basis, swapping the A site metal of perovskite (ABO_3) to a lower-valent metal (*e.g.* from $LaCoO_3$ to $SrCoO_3$) results in a down-shift of Fermi level (Fig. 4d). When the Fermi level crosses the top of the O 2p states and moves below the O_2/H_2O redox energy (1.23 eV), oxidation of lattice oxygen becomes more thermodynamically

favoured than that of water (Fig. 4e).[168,180] The above explains why OER catalysts with low overpotential are mostly oxides with high valence metals. Such high valence metal sites are intrinsically unstable under ambient conditions, and are therefore often generated *in situ* under applied OER-relevant potential.

The existence of high valence metal sites (*i.e.* Ni^{4+}) during the OER has been confirmed using *in situ* soft XAS,[181] and the generation of such sites usually results from dissolution of other constituent metals therefore forming a defect-rich surface layer.[96,181–187] For example, perovskite hydroxide $CoSn(OH)_6$ was used as a pre-catalyst, and *in situ* transformed into a highly active OER catalyst *via* electrochemical etching (galvanostatic activation in the reference) of Sn component.[182] As another example, the pre-catalyst of La- and Mn-codoped cobalt spinel was transformed into a surface-defect-rich OER catalyst upon leaching of lanthanum content as La^{3+}.[183] It is also proposed that the M–O–M motifs (M = Fe, Co, Ni) within the *in situ* formed amorphous layers of metal oxyhydroxide function as the active sites for enhanced OER activity.[188] Under the harsh reaction environment of acidic OER, even iridium suffers from notable dissolution from the pre-catalyst. Through manipulation of the composition of Ir-based perovskite pre-catalysts and dissolution/electrochemical test conditions, it is proposed that the IrO_x amorphous layer formed *in situ* through continuous dissolution/precipitation functions as the true catalyst determining the OER performance.[189]

A self-healing electrocatalyst spontaneously regenerates its active sites under the operating conditions (*i.e.* dynamic equilibrium of multiple reactions).[190,191] In such a system, therefore, both processes of loss and regeneration of active sites are continuous and dynamic throughout the course of reaction.[190,191] Distinction should be made between self-healing and self-repairing (Fig. 5a), where in the latter, the regeneration of active sites only occurs when the cell operation is stopped (*e.g.* at open-circuit).[190,191] Based on the above, the reported on–off electrolysis[192] and the self-assembled metal–organic macrocycle catalyst[193] in ECO_2R are self-repairing at best. Compared to pulse electrolysis, self-repairing catalysts offer notable merits by removing sophisticated control and continuous power supply. The more desirable self-healing catalysts, however, are yet to be reported for ECO_2R. Self-healing catalysts in OER operate based on parallel dissolution and precipitation of metal oxide clusters (Fig. 5b).[190]

Selection of a pre-catalyst metal (*e.g.* Mn, Co, and Ni) cation and solution phase oxyanion (*e.g.* phosphate, methylphosphonate, and borate) pair is crucial to ensure the self-healing feature of the electrocatalytic system. An appropriate cation-oxyanion pair allows dissolved cations to precipitate as oxides/oxyhydroxides, and the size of the latter is regulated *via* metallate capping formed from the reaction between oxyanions and dissolved metal cations.[190,194] The pre-catalysts of such self-healing OER catalysts usually contain a metal component that upon restructuring serves as a porous conductive support (*e.g.* indium tin oxide,[194] fluorine-doped tin oxide,[195] lead oxide,[196] *etc.*) to ensure facile electronic and ionic conducting pathways. In HER, although not specifically stated as a

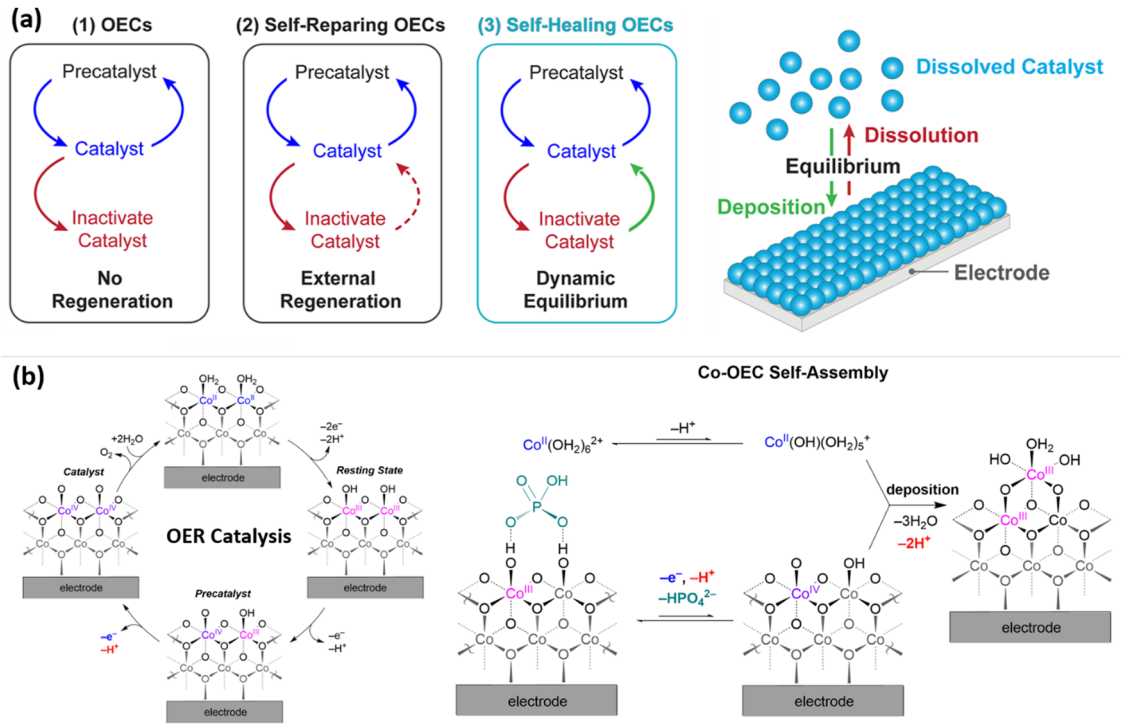

Fig. 5 Comparison between conventional oxygen evolution catalysts (OECs), self-repairing OECs, and self-healing OECs. (a) Summary and schematic illustration of the operating principle of self-healing OECs. (b) Mechanistic schemes of the OER on conventional catalysts (left) *versus* that on self-healing OECs (Co-OEC assembly, right). Figures adapted with permission from ref. 190. Copyright 2022. Springer Nature.

self-healing system, certain metal alloys also display self-healing properties, where the dissolved molybdenum cations from pre-catalysts polymerize to form polymolybdate which stabilizes the *in situ* generated catalyst with enhanced HER activity.[197] It has been demonstrated that reversible *in situ* restructuring can be achieved, which allows the catalyst to convert between two active forms depending on the operating condition (*i.e.* a bifunctional electrocatalyst).[198,199] The pre-catalysts of such bifunctional electrocatalysts are usually prepared *via* electrodeposition in pH-buffered oxyanion solution, where the incorporated phosphorus[198] or boron[199] content in the near surface region facilitates the ensuing reversible restructuring. In electrochemical nitrate reduction reaction, amorphous surface layers resulting from *in situ* restructuring are often observed, which deliver improved faradaic efficiencies towards ammonia *via* stabilization of *NOH intermediates[200,201] and/or suppression of HER,[202,203] or through improved adsorption to nitrate anions.[204]

The above two sections have discussed the positive and negative impacts of *in situ* restructuring of catalysts on the outcome of electrochemical process. A tabular comparison summarizing the discussion and examples presented is shown in Table 1.

4. Perspectives and outlook

The fundamental origins and impacts of *in situ* restructuring of catalysts on electrochemical processes have been reviewed. Designs of pre-catalysts and pre-treatment/activation methods have found notable success, but the long-term operational stability of some of these strategies developed in a laboratory scale is questionable when advancing to industrial scales. Design strategies of pre-catalysts (*e.g.* alloying, doping, molecular tuning, size and facet engineering, oxidation state, defect engineering, *etc.*) have been covered in excellent reviews,[27,28,31,36] and the effectiveness of these approaches rely on controlled/guided restructuring towards the most active and/or selective form of the electrocatalyst. In terms of manipulating restructuring through pre-treatment/activation methods, some of the proposed approaches, such as pulse electrolysis[179,207] and *in situ* electrochemical dealloying,[52,55] still face critical challenges in industrially-relevant setups, due to the impracticality of implementing three-electrode systems and the stability issue related to the leached metals, respectively. We'd like to present four perspectives and outlooks regarding the application of *in situ* restructuring of electrocatalysts in practical industrial settings.

(1) Pulse electrolysis has found success in ECO_2R in regulating active sites to generate targeted products with improved stability and/or selectivity when the restructuring process is reversible under electrochemical conditions. However, it is worth noting that such a technique faces challenges in scaling up towards commercialization. A process that relies on the precise control of the potential of an electrode requires the implementation of a reference electrode (*i.e.* a three-electrode cell). Such a half-cell approach has completely disregarded possible impacts of pulse on the efficiency and stability of counter electrode catalyst, which are equally important in an electrochemical process. Therefore, in large-scale industrial electrochemical processes, the long-term use of reference electrodes throughout the operation is very rare if not non-existent. Instead, constant cell voltage or current is the most practiced mode of operation due to its simplicity and practicality. In the Hall–Héroult electrochemical process for aluminium production for example, constant voltage electrolysis is maintained by adjusting the electrolyte resistance (*i.e.* distance between the anode and cathode).[208] In chlor-alkali electrolysis, a constant current is applied and the cell voltage is monitored, which serves as an indicator for reactant (*i.e.* brine solution) flowrate adjustment to keep the operation at the highest energy efficiency.[209,210]

(2) Approaches to inducing *in situ* restructuring of electrocatalysts towards a more active/selective form and stabilizing them for a prolonged period of time under practical conditions (including transient operation such as start-up and shut-down) are essential to the development of energy-efficient and durable electrochemical processes. Revisiting the concept of promoter discussed at the beginning of this article, the introduction of appropriate species into the electrolyte together with the pre-catalyst to form a catalytic system has shown substantial promise in the OER (*e.g.* phosphate–Co[194]), HER

Table 1 Summary of positive and negative impacts of catalyst restructuring on example electrocatalytic reactions

Electrocatalytic reaction	Example catalyst	Restructuring event	Negative impact	Positive impact
ORR	PtM (M = Co, Ni, Cu, Se, *etc.*)	Metal leaching	Dissolved metal cations poison the ionomer and membrane in fuel cells.[98,99] Fenton-like reaction leading to membrane degradation[100]	Under the right conditions, the resulting Pt-rich shell offers higher specific activity[53,57,157]
OER	Metal oxides	Metal leaching	Loss of active sites. Corrosion and amorphous layer formation compromise the mechanical integrity of the electrode[29,30,32]	Under the right combination of electrolyte and (mixed) metal oxide catalyst, self-healing can be achieved with high activity and stability[190,194,196]
ECO_2R	Cu-based particles	Formation of an amorphous surface layer	At long time scales, undercoordinated sites are consumed through Ostwald ripening and other processes, eventually leading to decreased activity and selectivity[43,66,117]	At short time scales, the generated undercoordinated sites improve the selectivity towards multi-carbon products[20,205]
HER	Transition metal chalcogenides	Formation of the restructured surface layer	Prolonged operation favors the formation of highly crystalline MoS_2 domains, or inactive oxides/oxyhydroxides on the surface, which deactivates the catalyst[206]	*In situ* formation of an amorphous layer exposes highly active sites[162,206]

(polymolybdate–Ni[197]), ECO_2R (imidazolium-based-ionic-liquid-Ag,[211] functionalized-iron-porphine-Cu[212]), and e-NRR ($LiClO_4$–Cu[213]). The fact that even the state-of-the-art Haber–Bosch process relies on the addition of a promoter suggests that this approach towards regulated restructuring deserves more research attention in electrocatalysis.

(3) The concept of self-healing catalysts, where highly active/selective sites are generated, consumed upon reaction, and renewed constantly, provides prospects for an energy-efficient and durable process. Considering that efficient and stable OER has been achieved under harsh conditions (*e.g.* 80 °C and pH = 1) through a self-healing catalyst,[196] the next step towards commercialization should be the improvement in impurity tolerance of the catalyst system, and insights can be obtained from seawater electrolysis.[214,215] How self-healing can be realized for reactions other than OER and HER, which will require appropriate selection and pairing of solution phase species and catalyst metal components, is still an area rarely explored.

(4) In order to develop more reliable control of *in situ* restructuring of electrocatalysts to our advantage, advances in characterization techniques on electrochemical interfaces and a rigorous understanding of electrokinetics and other potential activity/selectivity descriptors beyond adsorption energy[216] should propel the field greatly. Advances in the above areas will allow us greater access to the *in situ* restructuring of more complex electrocatalytic reactions, such as electrosynthesis of ammonia through co-reduction of dinitrogen[217–219] or nitrate[220,221] with CO_2. The formation of the C–N bond requires the atomic-scale proximity of intrinsically different sites (*i.e.* strong $*N_2$ or *NOH binding *vs.* strong $*CO_2$ binding), which poses challenges in catalyst synthesis. The greatly increased number of possible intermediates and side reactions further complicates the *in situ* restructuring scenario. Considering the fact that the catalyst restructuring in the e-NRR is still masked by the dominant competing HER, a breakthrough in characterization techniques is required to elucidate the structural evolution attributed to the electrochemical C–N coupling from CO_2 and N_2.

In summary, the dynamic nature of electrocatalyst surface has introduced both challenges and opportunities to the industrial applications of electrochemical processes. *In situ* restructuring impacts negatively the electrocatalytic outcome when the evolved stable form of the catalyst during operation is of low activity and/or selectivity, or when other device components become poisoned or failed in the course of restructuring. Positive impacts may also be observed on restructured electrocatalysts if the stable form delivers improved activity and/or selectivity than the pre-catalysts. The authors hope that this review article will inspire researchers to advance electrochemical technologies and to ensure access to affordable, reliable and sustainable energy for all.

Data availability

No primary research results, software or code have been included and no new data were generated or analysed as part of this review.

Conflicts of interest

There are no conflicts to declare.

Acknowledgements

This work was supported by the Australian Research Council (ARC) Centre of Excellence for Green Electrochemical Transformation of Carbon Dioxide (CE230100017), the ARC Research Hub for Carbon Utilisation and Recycling (IH220100012), an ARC Discovery Project grant (DP220100316), and a Monash-Woodside Energy Partnership grant. Open access publishing was facilitated by Monash University, as part of the Royal Society of Chemistry – Monash University agreement *via* the Council of Australian University Librarians.

References

1 C. Vogt and B. M. Weckhuysen, *Nat. Rev. Chem.*, 2022, **6**, 89–111.
2 L. Liu and A. Corma, *Nat. Rev. Chem.*, 2021, **5**, 256–276.
3 T. Luttrell, S. Halpegamage, J. Tao, A. Kramer, E. Sutter and M. Batzill, *Sci. Rep.*, 2014, **4**, 4043.
4 M. A. Henderson, *Surf. Sci. Rep.*, 2011, **66**, 185–297.
5 M. Liu, Y. Pang, B. Zhang, P. De Luna, O. Voznyy, J. Xu, X. Zheng, C. T. Dinh, F. Fan and C. Cao, *Nature*, 2016, **537**, 382–386.
6 F. Li, X. V. Medvedeva, J. J. Medvedev, E. Khairullina, H. Engelhardt, S. Chandrasekar, Y. Guo, J. Jin, A. Lee and H. Thérien-Aubin, *Nat. Catal.*, 2021, **4**, 479–487.
7 G. J. Hutchings, *Catal. Lett.*, 2001, **75**, 1–12.
8 H. Liu, *Chin. J. Catal.*, 2014, **35**, 1619–1640.
9 J. Folke, K. Dembélé, F. Girgsdies, H. Song, R. Eckert, S. Reitmeier, A. Reitzmann, R. Schlögl, T. Lunkenbein and H. Ruland, *Catal. Today*, 2022, **387**, 12–22.
10 D. R. Strongin and G. A. Somorjai, *J. Catal.*, 1988, **109**, 51–60.
11 Y. Kwon, Y. Lum, E. L. Clark, J. W. Ager and A. T. Bell, *ChemElectroChem*, 2016, **3**, 1012–1019.
12 D. Gao, F. Scholten and B. Roldan Cuenya, *ACS Catal.*, 2017, **7**, 5112–5120.
13 A. S. Varela, W. Ju, T. Reier and P. Strasser, *ACS Catal.*, 2016, **6**, 2136–2144.
14 P.-P. Yang, X.-L. Zhang, P. Liu, D. J. Kelly, Z.-Z. Niu, Y. Kong, L. Shi, Y.-R. Zheng, M.-H. Fan and H.-J. Wang, *J. Am. Chem. Soc.*, 2023, **145**, 8714–8725.
15 P. Liu, H. Liu, S. Zhang, J. Wang and C. Wang, *Electrochim. Acta*, 2020, **354**, 136753.
16 S. Lee, D. Kim and J. Lee, *Angew. Chem.*, 2015, **127**, 14914–14918.
17 C. W. Li and M. W. Kanan, *J. Am. Chem. Soc.*, 2012, **134**, 7231–7234.
18 C. W. Li, J. Ciston and M. W. Kanan, *Nature*, 2014, **508**, 504–507.
19 D. Ren, Y. Deng, A. D. Handoko, C. S. Chen, S. Malkhandi and B. S. Yeo, *ACS Catal.*, 2015, **5**, 2814–2821.
20 X. Wang, K. Klingan, M. Klingenhof, T. Möller, J. Ferreira de Araújo, I. Martens, A. Bagger, S. Jiang, J. Rossmeisl and H. Dau, *Nat. Commun.*, 2021, **12**, 794.
21 T. Möller, F. Scholten, T. N. Thanh, I. Sinev, J. Timoshenko, X. Wang, Z. Jovanov, M. Gliech, B. Roldan Cuenya and A. S. Varela, *Angew. Chem.*, 2020, **132**, 18130–18139.
22 W. Fu, Z. Liu, T. Wang, J. Liang, S. Duan, L. Xie, J. Han and Q. Li, *ACS Sustainable Chem. Eng.*, 2020, **8**, 15223–15229.
23 C. S. Chen, A. D. Handoko, J. H. Wan, L. Ma, D. Ren and B. S. Yeo, *Catal. Sci. Technol.*, 2015, **5**, 161–168.
24 A. S. Malkani, M. Dunwell and B. Xu, *ACS Catal.*, 2018, **9**, 474–478.
25 K. Jiang, Y. Huang, G. Zeng, F. M. Toma, W. A. Goddard III and A. T. Bell, *ACS Energy Lett.*, 2020, **5**, 1206–1214.
26 J. E. Pander III, D. Ren, Y. Huang, N. W. X. Loo, S. H. L. Hong and B. S. Yeo, *ChemElectroChem*, 2018, **5**, 219–237.
27 J. Zhang, S. Xia, Y. Wang, J. Wu and Y. Wu, *iScience*, 2024, **27**, 110005.

28 L. Wang, Q. Meng, M. Xiao, C. Liu, W. Xing and J. Zhu, *Renewables*, 2024, **2**, 272–296.
29 J. Wang, *Chem*, 2023, **9**, 1645–1657.
30 J. Wang, *Curr. Opin. Electrochem.*, 2023, **39**, 101304.
31 L. Gao, X. Cui, C. D. Sewell, J. Li and Z. Lin, *Chem. Soc. Rev.*, 2021, **50**, 8428–8469.
32 J. Chen, H. Chen, T. Yu, R. Li, Y. Wang, Z. Shao and S. Song, *Electrochem. Energy Rev.*, 2021, **4**, 566–600.
33 Y. Zhu, T.-R. Kuo, Y.-H. Li, M.-Y. Qi, G. Chen, J. Wang, Y.-J. Xu and H. M. Chen, *Energy Environ. Sci.*, 2021, **14**, 1928–1958.
34 B. Hasa, Y. Zhao and F. Jiao, *Annu. Rev. Chem. Biomol. Eng.*, 2023, **14**, 165–185.
35 H. Jiang, Q. He, Y. Zhang and L. Song, *Acc. Chem. Res.*, 2018, **51**, 2968–2977.
36 W. Wang, J. Duan, Y. Liu and T. Zhai, *Adv. Mater.*, 2022, **34**, 2110699.
37 C. Xia, F.-M. Li, C. He, S. Zaman, W. Guo and B. Y. Xia, *Fundam. Res.*, 2024, DOI: 10.1016/j.fmre.2024.04.017.
38 Y. Huang, W. Quan, H. Yao, R. Yang, Z. Hong and Y. Lin, *Inorg. Chem. Front.*, 2023, **10**, 352–369.
39 G. Nichols, S. Byard, M. J. Bloxham, J. Botterill, N. J. Dawson, A. Dennis, V. Diart, N. C. North and J. D. Sherwood, *J. Pharm. Sci.*, 2002, **91**, 2103–2109.
40 A. D. McNaught and A. Wilkinson, *IUPAC compendium of chemical terminology*, Royal Society of Chemistry, 1997.
41 E. Goudeli and S. E. Pratsinis, *AIChE J.*, 2016, **62**, 589–598.
42 Z. Zhang, Z. Wang, S. He, C. Wang, M. Jin and Y. Yin, *Chem. Sci.*, 2015, **6**, 5197–5203.
43 J. Vavra, T. H. Shen, D. Stoian, V. Tileli and R. Buonsanti, *Angew. Chem.*, 2021, **133**, 1367–1374.
44 H. Wu, H. Yu, Y.-L. Chow, P. A. Webley and J. Zhang, *Adv. Mater.*, 2024, **36**, 2403217.
45 W. Lai, Y. Qiao, Y. Wang and H. Huang, *Adv. Mater.*, 2023, **35**, 2306288.
46 J. Chen and L. Wang, *Adv. Mater.*, 2022, **34**, 2103900.
47 S. Cherevko, S. Geiger, O. Kasian, N. Kulyk, J.-P. Grote, A. Savan, B. R. Shrestha, S. Merzlikin, B. Breitbach, A. Ludwig and K. J. J. Mayrhofer, *Catal. Today*, 2016, **262**, 170–180.
48 J. Choi, J. Cho, C.-W. Roh, B.-S. Kim, M. S. Choi, H. Jeong, H. C. Ham and H. Lee, *Appl. Catal., B*, 2019, **247**, 142–149.
49 T.-Y. Jeon, S. K. Kim, N. Pinna, A. Sharma, J. Park, S. Y. Lee, H. C. Lee, S.-W. Kang, H.-K. Lee and H. H. Lee, *Chem. Mater.*, 2016, **28**, 1879–1887.
50 C. Roiron, V. Martin, K. Kumar, L. Dubau and F. Maillard, *Electrochim. Acta*, 2024, **477**, 143760.
51 K. Jayasayee, J. A. R. V. Veen, T. G. Manivasagam, S. Celebi, E. J. M. Hensen and F. A. de Bruijn, *Appl. Catal., B*, 2012, **111–112**, 515–526.
52 W. Niu, S. Pakhira, G. Cheng, F. Zhao, N. Yao, J. L. Mendoza-Cortes and B. E. Koel, *Nat. Mater.*, 2024, **23**, 1704–1711.
53 V. R. Stamenkovic, B. S. Mun, K. J. J. Mayrhofer, P. N. Ross and N. M. Markovic, *J. Am. Chem. Soc.*, 2006, **128**, 8813–8819.
54 L. Gan, M. Heggen, R. O'Malley, B. Theobald and P. Strasser, *Nano Lett.*, 2013, **13**, 1131–1138.
55 P. Strasser and S. Kühl, *Nano Energy*, 2016, **29**, 166–177.
56 I. Khalakhan, M. Bogar, M. Vorokhta, P. Kúš, Y. Yakovlev, M. Dopita, D. J. S. Sandbeck, S. Cherevko, I. Matolínová and H. Amenitsch, *ACS Appl. Mater. Interfaces*, 2020, **12**, 17602–17610.
57 C. Cui, L. Gan, M. Heggen, S. Rudi and P. Strasser, *Nat. Mater.*, 2013, **12**, 765–771.
58 Y. Zhao, X. Chang, A. S. Malkani, X. Yang, L. Thompson, F. Jiao and B. Xu, *J. Am. Chem. Soc.*, 2020, **142**, 9735–9743.
59 S. H. Lee, J. C. Lin, M. Farmand, A. T. Landers, J. T. Feaster, J. E. Avilés Acosta, J. W. Beeman, Y. Ye, J. Yano and A. Mehta, *J. Am. Chem. Soc.*, 2020, **143**, 588–592.
60 T. Wirtanen, T. Prenzel, J.-P. Tessonnier and S. R. Waldvogel, *Chem. Rev.*, 2021, **121**, 10241–10270.
61 A. I. Yanson, P. Rodriguez, N. Garcia-Araez, R. V. Mom, F. D. Tichelaar and M. T. Koper, *Angew. Chem.*, 2011, **123**, 6470–6474.
62 B. Vanrenterghem, M. Bele, F. Zepeda, M. Šala, N. Hodnik and T. Breugelmans, *Appl. Catal., B*, 2018, **226**, 396–402.
63 S. Sarkar and S. C. Peter, *Inorg. Chem. Front.*, 2018, **5**, 2060–2080.
64 C. Liu, F. Chen, B.-H. Zhao, Y. Wu and B. Zhang, *Nat. Rev. Chem.*, 2024, **8**, 277–293.
65 A. Zalineeva, S. Baranton, C. Coutanceau and G. Jerkiewicz, *Sci. Adv.*, 2017, **3**, e1600542.
66 J. Vavra, G. P. L. Ramona, F. Dattila, A. Kormányos, T. Priamushko, P. P. Albertini, A. Loiudice, S. Cherevko, N. Lopéz and R. Buonsanti, *Nat. Catal.*, 2024, **7**, 89–97.
67 L. Xu, K. G. Papanikolaou, B. A. Lechner, L. Je, G. A. Somorjai, M. Salmeron and M. Mavrikakis, *Science*, 2023, **380**, 70–76.
68 B. Eren, D. Zherebetskyy, L. L. Patera, C. H. Wu, H. Bluhm, C. Africh, L.-W. Wang, G. A. Somorjai and M. Salmeron, *Science*, 2016, **351**, 475–478.
69 M. Roiaz, L. Falivene, C. Rameshan, L. Cavallo, S. M. Kozlov and G. N. Rupprechter, *J. Phys. Chem. C*, 2018, **123**, 8112–8121.
70 P. L. Hansen, J. B. Wagner, S. Helveg, J. R. Rostrup-Nielsen, B. S. Clausen and H. Topsøe, *Science*, 2002, **295**, 2053–2055.
71 B. Eren and M. Salmeron, *J. Phys. Chem. C*, 2018, **123**, 8171–8176.
72 A. A. Gokhale, J. A. Dumesic and M. Mavrikakis, *J. Am. Chem. Soc.*, 2008, **130**, 1402–1414.
73 W. D. Williams, M. Shekhar, W.-S. Lee, V. Kispersky, W. N. Delgass, F. H. Ribeiro, S. M. Kim, E. A. Stach, J. T. Miller and L. F. Allard, *J. Am. Chem. Soc.*, 2010, **132**, 14018–14020.
74 S. Kuld, M. Thorhauge, H. Falsig, C. F. Elkjær, S. Helveg, I. Chorkendorff and J. Sehested, *Science*, 2016, **352**, 969–974.
75 F. Wang, J. Ma, G. He, M. Chen, C. Zhang and H. He, *ACS Catal.*, 2018, **8**, 2670–2682.
76 L. Xu and M. Mavrikakis, *JACS Au*, 2023, **3**, 2216–2225.
77 H. Matsushima, C. Haak, A. Taranovskyy, Y. Gründer and O. M. Magnussen, *Phys. Chem. Chem. Phys.*, 2010, **12**, 13992–13998.
78 H. Matsushima, A. Taranovskyy, C. Haak, Y. Gründer and O. M. Magnussen, *J. Am. Chem. Soc.*, 2009, **131**, 10362–10363.
79 R. Amirbeigiarab, J. Tian, A. Herzog, C. Qiu, A. Bergmann, B. Roldan Cuenya and O. M. Magnussen, *Nat. Catal.*, 2023, **6**, 837–846.
80 P. Wilde, P. B. O'Mara, J. R. Junqueira, T. Tarnev, T. M. Benedetti, C. Andronescu, Y.-T. Chen, R. D. Tilley, W. Schuhmann and J. J. Gooding, *Chem. Sci.*, 2021, **12**, 4028–4033.
81 L. Xu, M. Rebarchik, S. Bhandari and M. Mavrikakis, *Surf. Sci.*, 2024, 122613, DOI: 10.1016/j.susc.2024.122613.
82 Q. Zhang, Z. Song, X. Sun, Y. Liu, J. Wan, S. B. Betzler, Q. Zheng, J. Shangguan, K. C. Bustillo, P. Ercius, P. Narang, Y. Huang and H. Zheng, *Nature*, 2024, **630**, 643–647.
83 E. L. Clark, C. Hahn, T. F. Jaramillo and A. T. Bell, *J. Am. Chem. Soc.*, 2017, **139**, 15848–15857.
84 A. Bagger, W. Ju, A. S. Varela, P. Strasser and J. Rossmeisl, *ChemPhysChem*, 2017, **18**, 3266–3273.
85 D. Karapinar, N. T. Huan, N. Ranjbar Sahraie, J. Li, D. Wakerley, N. Touati, S. Zanna, D. Taverna, L. H. Galvão Tizei and A. Zitolo, *Angew. Chem., Int. Ed.*, 2019, **58**, 15098–15103.
86 H. Xu, D. Rebollar, H. He, L. Chong, Y. Liu, C. Liu, C.-J. Sun, T. Li, J. V. Muntean and R. E. Winans, *Nat. Energy*, 2020, **5**, 623–632.
87 Z. Weng, Y. Wu, M. Wang, J. Jiang, K. Yang, S. Huo, X.-F. Wang, Q. Ma, G. W. Brudvig and V. S. Batista, *Nat. Commun.*, 2018, **9**, 415.
88 X. Bai, X. Zhao, Y. Zhang, C. Ling, Y. Zhou, J. Wang and Y. Liu, *J. Am. Chem. Soc.*, 2022, **144**, 17140–17148.
89 C. M. Gunathunge, X. Li, J. Li, R. P. Hicks, V. J. Ovalle and M. M. Waegele, *J. Phys. Chem. C*, 2017, **121**, 12337–12344.
90 S. Mu, H. Lu, Q. Wu, L. Li, R. Zhao, C. Long and C. Cui, *Nat. Commun.*, 2022, **13**, 3694.
91 S. Fierro, T. Nagel, H. Baltruschat and C. Comninellis, *Electrochem. Commun.*, 2007, **9**, 1969–1974.
92 O. Diaz-Morales, F. Calle-Vallejo, C. de Munck and M. T. M. Koper, *Chem. Sci.*, 2013, **4**, 2334–2343.
93 R. Kötz, S. Stucki, D. Scherson and D. M. Kolb, *J. Electroanal. Chem. Interfacial Electrochem.*, 1984, **172**, 211–219.
94 N. Danilovic, R. Subbaraman, K.-C. Chang, S. H. Chang, Y. J. Kang, J. Snyder, A. P. Paulikas, D. Strmcnik, Y.-T. Kim, D. Myers, V. R. Stamenkovic and N. M. Markovic, *J. Phys. Chem. Lett.*, 2014, **5**, 2474–2478.
95 S. Cherevko, A. R. Zeradjanin, A. A. Topalov, N. Kulyk, I. Katsounaros and K. J. J. Mayrhofer, *ChemCatChem*, 2014, **6**, 2219–2223.
96 E. Fabbri, M. Nachtegaal, T. Binninger, X. Cheng, B.-J. Kim, J. Durst, F. Bozza, T. Graule, R. Schäublin, L. Wiles, M. Pertoso, N. Danilovic, K. E. Ayers and T. J. Schmidt, *Nat. Mater.*, 2017, **16**, 925–931.

97 M. Dunwell, Q. Lu, J. M. Heyes, J. Rosen, J. G. Chen, Y. Yan, F. Jiao and B. Xu, *J. Am. Chem. Soc.*, 2017, **139**, 3774–3783.
98 S. Cherevko, N. Kulyk and K. J. J. Mayrhofer, *Nano Energy*, 2016, **29**, 275–298.
99 A. Kongkanand, N. P. Subramanian, Y. Yu, Z. Liu, H. Igarashi and D. A. Muller, *ACS Catal.*, 2016, **6**, 1578–1583.
100 P. C. Okonkwo, I. Ben Belgacem, W. Emori and P. C. Uzoma, *Int. J. Hydrogen Energy*, 2021, **46**, 27956–27973.
101 D. K. Pattadar and F. P. Zamborini, *Langmuir*, 2019, **35**, 16416–16426.
102 R. L. Borup, A. Kusoglu, K. C. Neyerlin, R. Mukundan, R. K. Ahluwalia, D. A. Cullen, K. L. More, A. Z. Weber and D. J. Myers, *Curr. Opin. Electrochem.*, 2020, **21**, 192–200.
103 Z. Xu, H. Zhang, H. Zhong, Q. Lu, Y. Wang and D. Su, *Appl. Catal., B*, 2012, **111–112**, 264–270.
104 H. Wu, F. Xiao, J. Wang, M. Gu and M. Shao, *Nano Res.*, 2024, **17**, 8772–8784.
105 R. Sgarbi, W. Ait Idir, Q. Labarde, M. Mermoux, P. Wu, J. Mainka, J. Dillet, C. Marty, F. Micoud, O. Lottin and M. Chatenet, *Ind. Chem. Mater.*, 2023, **1**, 501–515.
106 E. L. Clark, R. Nielsen, J. E. Sørensen, J. L. Needham, B. Seger and I. Chorkendorff, *ACS Energy Lett.*, 2023, **8**, 4414–4420.
107 Y. Guo, S. Mei, K. Yuan, D.-J. Wang, H.-C. Liu, C.-H. Yan and Y.-W. Zhang, *ACS Catal.*, 2018, **8**, 6203–6215.
108 J. C. Matsubu, V. N. Yang and P. Christopher, *J. Am. Chem. Soc.*, 2015, **137**, 3076–3084.
109 F. Wang, C. Li, X. Zhang, M. Wei, D. G. Evans and X. Duan, *J. Catal.*, 2015, **329**, 177–186.
110 E. Gioria, L. Duarte-Correa, N. Bashiri, W. Hetaba, R. Schomaecker and A. Thomas, *Nanoscale Adv.*, 2021, **3**, 3454–3459.
111 K. Larmier, W. C. Liao, S. Tada, E. Lam, R. Verel, A. Bansode, A. Urakawa, A. Comas-Vives and C. Copéret, *Angew. Chem., Int. Ed.*, 2017, **56**, 2318–2323.
112 J. Li, Y. He, L. Tan, P. Zhang, X. Peng, A. Oruganti, G. Yang, H. Abe, Y. Wang and N. Tsubaki, *Nat. Catal.*, 2018, **1**, 787–793.
113 Y. Qiao, G. Kastlunger, R. C. Davis, C. A. G. Rodriguez, A. Vishart, W. Deng, Q. Xu, S. Li, P. Benedek and J. Chen, *ACS Catal.*, 2023, **13**, 9379–9391.
114 H. S. Jeon, J. Timoshenko, F. Scholten, I. Sinev, A. Herzog, F. T. Haase and B. Roldan Cuenya, *J. Am. Chem. Soc.*, 2019, **141**, 19879–19887.
115 S. Kunze, P. Grosse, M. Bernal Lopez, I. Sinev, I. Zegkinoglou, H. Mistry, J. Timoshenko, M. Y. Hu, J. Zhao and E. E. Alp, *Angew. Chem.*, 2020, **132**, 22856–22863.
116 R. M. Arán-Ais, F. Scholten, S. Kunze, R. Rizo and B. Roldan Cuenya, *Nat. Energy*, 2020, **5**, 317–325.
117 Y. Yang, S. Louisia, S. Yu, J. Jin, I. Roh, C. Chen, M. V. Fonseca Guzman, J. Feijóo, P.-C. Chen and H. Wang, *Nature*, 2023, **614**, 262–269.
118 R. M. Arán-Ais, R. Rizo, P. Grosse, G. Algara-Siller, K. Dembélé, M. Plodinec, T. Lunkenbein, S. W. Chee and B. R. Cuenya, *Nat. Commun.*, 2020, **11**, 3489.
119 P. Grosse, A. Yoon, C. Rettenmaier, A. Herzog, S. W. Chee and B. Roldan Cuenya, *Nat. Commun.*, 2021, **12**, 6736.
120 G. Qing, R. Ghazfar, S. T. Jackowski, F. Habibzadeh, M. M. Ashtiani, C.-P. Chen, M. R. Smith, III and T. W. Hamann, *Chem. Rev.*, 2020, **120**, 5437–5516.
121 D. R. MacFarlane, P. V. Cherepanov, J. Choi, B. H. R. Suryanto, R. Y. Hodgetts, J. M. Bakker, F. M. Ferrero Vallana and A. N. Simonov, *Joule*, 2020, **4**, 1186–1205.
122 Y. Wang, C. Wang, M. Li, Y. Yu and B. Zhang, *Chem. Soc. Rev.*, 2021, **50**, 6720–6733.
123 D. Liu, L. Qiao, S. Peng, H. Bai, C. Liu, W. F. Ip, K. H. Lo, H. Liu, K. W. Ng, S. Wang, X. Yang and H. Pan, *Adv. Funct. Mater.*, 2023, **33**, 2303480.
124 S. Han, H. Li, T. Li, F. Chen, R. Yang, Y. Yu and B. Zhang, *Nat. Catal.*, 2023, **6**, 402–414.
125 K. Fan, W. Xie, J. Li, Y. Sun, P. Xu, Y. Tang, Z. Li and M. Shao, *Nat. Commun.*, 2022, **13**, 7958.
126 A. Biswas, S. Nandi, N. Kamboj, J. Pan, A. Bhowmik and R. S. Dey, *ACS Nano*, 2021, **15**, 20364–20376.
127 D. Gupta, A. Kafle, S. Kaur, P. P. Mohanty, T. Das, S. Chakraborty, R. Ahuja and T. C. Nagaiah, *J. Mater. Chem. A*, 2022, **10**, 20616–20625.
128 U. K. Ghorai, S. Paul, B. Ghorai, A. Adalder, S. Kapse, R. Thapa, A. Nagendra and A. Gain, *ACS Nano*, 2021, **15**, 5230–5239.
129 J. Wang, B. Huang, Y. Ji, M. Sun, T. Wu, R. Yin, X. Zhu, Y. Li, Q. Shao and X. Huang, *Adv. Mater.*, 2020, **32**, 1907112.
130 B. H. R. Suryanto, H.-L. Du, D. Wang, J. Chen, A. N. Simonov and D. R. MacFarlane, *Nat. Catal.*, 2019, **2**, 290–296.
131 Y. Wang, T. Li, Y. Yu and B. Zhang, *Angew. Chem., Int. Ed.*, 2022, **61**, e202115409.
132 S. Paul, A. Adalder, N. Barman, R. Thapa, A. Bera, K. Mitra and U. K. Ghorai, *Adv. Funct. Mater.*, 2024, **34**, 2408314.
133 A. Adalder, S. Paul, B. Ghorai, S. Kapse, R. Thapa, A. Nagendra and U. K. Ghorai, *ACS Appl. Mater. Interfaces*, 2023, **15**, 34642–34650.
134 R. Singh, A. Biswas, N. Barman, M. Iqbal, R. Thapa and R. S. Dey, *Small*, 2024, **20**, 2406718.
135 J. Liu and L. Guo, *Matter*, 2021, **4**, 2850–2873.
136 F. Lv, N. Han, Y. Qiu, X. Liu, J. Luo and Y. Li, *Coord. Chem. Rev.*, 2020, **422**, 213435.
137 W. Fan, Z. Duan, W. Liu, R. Mehmood, J. Qu, Y. Cao, X. Guo, J. Zhong and F. Zhang, *Nat. Commun.*, 2023, **14**, 1426.
138 S. Aralekallu, S. Hadimane, Shantharaja, M. Nemakal and L. Koodlur Sannegowda, *Fuel*, 2024, **361**, 130736.
139 R. Matheu, E. Gutierrez-Puebla, M. Á. Monge, C. S. Diercks, J. Kang, M. S. Prévot, X. Pei, N. Hanikel, B. Zhang and P. Yang, *J. Am. Chem. Soc.*, 2019, **141**, 17081–17085.
140 N. Han, Y. Wang, L. Ma, J. Wen, J. Li, H. Zheng, K. Nie, X. Wang, F. Zhao and Y. Li, *Chem*, 2017, **3**, 652–664.
141 J. Choi, P. Wagner, S. Gambhir, R. Jalili, D. R. MacFarlane, G. G. Wallace and D. L. Officer, *ACS Energy Lett.*, 2019, **4**, 666–672.
142 N. Corbin, J. Zeng, K. Williams and K. Manthiram, *Nano Res.*, 2019, **12**, 2093–2125.
143 L. Sun, V. Reddu, A. C. Fisher and X. Wang, *Energy Environ. Sci.*, 2020, **13**, 374–403.
144 N. Kornienko, Y. Zhao, C. S. Kley, C. Zhu, D. Kim, S. Lin, C. J. Chang, O. M. Yaghi and P. Yang, *J. Am. Chem. Soc.*, 2015, **137**, 14129–14135.
145 S. Lin, C. S. Diercks, Y.-B. Zhang, N. Kornienko, E. M. Nichols, Y. Zhao, A. R. Paris, D. Kim, P. Yang and O. M. Yaghi, *Science*, 2015, **349**, 1208–1213.
146 P. Shao, L. Yi, S. Chen, T. Zhou and J. Zhang, *J. Energy Chem.*, 2020, **40**, 156–170.
147 C. S. Diercks, Y. Liu, K. E. Cordova and O. M. Yaghi, *Nat. Mater.*, 2018, **17**, 301–307.
148 Y. An, X. Lv, W. Jiang, L. Wang, Y. Shi, X. Hang and H. Pang, *Green Chem. Eng.*, 2024, **5**, 187–204.
149 W. Zheng, M. Liu and L. Y. S. Lee, *ACS Catal.*, 2020, **10**, 81–92.
150 H. Jiang, Y. Lin, B. Chen, Y. Zhang, H. Liu, X. Duan, D. Chen and L. Song, *Mater. Today*, 2018, **21**, 602–610.
151 X. Cui, P. Ren, C. Ma, J. Zhao, R. Chen, S. Chen, N. P. Rajan, H. Li, L. Yu, Z. Tian and D. Deng, *Adv. Mater.*, 2020, **32**, 1908126.
152 C. Galeano, J. C. Meier, V. Peinecke, H. Bongard, I. Katsounaros, A. A. Topalov, A. Lu, K. J. Mayrhofer and F. Schüth, *J. Am. Chem. Soc.*, 2012, **134**, 20457–20465.
153 E. Padgett, V. Yarlagadda, M. E. Holtz, M. Ko, B. D. Levin, R. S. Kukreja, J. M. Ziegelbauer, R. N. Andrews, J. Ilavsky and A. Kongkanand, *J. Electrochem. Soc.*, 2019, **166**, F198.
154 J.-Y. Kim, D. Hong, J.-C. Lee, H. G. Kim, S. Lee, S. Shin, B. Kim, H. Lee, M. Kim and J. Oh, *Nat. Commun.*, 2021, **12**, 3765.
155 Y. Li, F. Cui, M. B. Ross, D. Kim, Y. Sun and P. Yang, *Nano Lett.*, 2017, **17**, 1312–1317.
156 Z. Zhang, G. Wen, D. Luo, B. Ren, Y. Zhu, R. Gao, H. Dou, G. Sun, M. Feng and Z. Bai, *J. Am. Chem. Soc.*, 2021, **143**, 6855–6864.
157 B. Han, C. E. Carlton, A. Kongkanand, R. S. Kukreja, B. R. Theobald, L. Gan, R. O'Malley, P. Strasser, F. T. Wagner and Y. Shao-Horn, *Energy Environ. Sci.*, 2015, **8**, 258–266.
158 A. A. Gewirth, J. A. Varnell and A. M. Diascro, *Chem. Rev.*, 2018, **118**, 2313–2339.
159 S. D. Bhoyate, J. Kim, F. M. de Souza, J. Lin, E. Lee, A. Kumar and R. K. Gupta, *Coord. Chem. Rev.*, 2023, **474**, 214854.
160 B. Yan, D. Krishnamurthy, C. H. Hendon, S. Deshpande, Y. Surendranath and V. Viswanathan, *Joule*, 2017, **1**, 600–612.
161 M. B. Stevens, M. E. Kreider, A. M. Patel, Z. Wang, Y. Liu, B. M. Gibbons, M. J. Statt, A. V. Ievlev, R. Sinclair, A. Mehta, R. C. Davis, J. K. Nørskov, A. Gallo, L. A. King and T. F. Jaramillo, *ACS Appl. Energy Mater.*, 2020, **3**, 12433–12446.

162 Y. Liu, J. Wu, K. P. Hackenberg, J. Zhang, Y. M. Wang, Y. Yang, K. Keyshar, J. Gu, T. Ogitsu, R. Vajtai, J. Lou, P. M. Ajayan, B. C. Wood and B. I. Yakobson, *Nat. Energy*, 2017, **2**, 17127.
163 X. Shang, K.-L. Yan, Y. Rao, B. Dong, J.-Q. Chi, Y.-R. Liu, X. Li, Y.-M. Chai and C.-G. Liu, *Nanoscale*, 2017, **9**, 12353–12363.
164 Y. Zhu, H.-C. Chen, C.-S. Hsu, T.-S. Lin, C.-J. Chang, S.-C. Chang, L.-D. Tsai and H. M. Chen, *ACS Energy Lett.*, 2019, **4**, 987–994.
165 A. Verdaguer-Casadevall, C. W. Li, T. P. Johansson, S. B. Scott, J. T. McKeown, M. Kumar, I. E. Stephens, M. W. Kanan and I. Chorkendorff, *J. Am. Chem. Soc.*, 2015, **137**, 9808–9811.
166 K. Yao, J. Li, A. Ozden, H. Wang, N. Sun, P. Liu, W. Zhong, W. Zhou, J. Zhou, X. Wang, H. Liu, Y. Liu, S. Chen, Y. Hu, Z. Wang, D. Sinton and H. Liang, *Nat. Commun.*, 1749, **2024**, 15.
167 S. Yu, S. Louisia and P. Yang, *JACS Au*, 2022, **2**, 562–572.
168 A. Grimaud, O. Diaz-Morales, B. Han, W. T. Hong, Y.-L. Lee, L. Giordano, K. A. Stoerzinger, M. T. M. Koper and Y. Shao-Horn, *Nat. Chem.*, 2017, **9**, 457–465.
169 H. Sun, L. Chen, L. Xiong, K. Feng, Y. Chen, X. Zhang, X. Yuan, B. Yang, Z. Deng and Y. Liu, *Nat. Commun.*, 2021, **12**, 6823.
170 Z. Li, L. Wang, T. Wang, L. Sun and W. Yang, *J. Am. Chem. Soc.*, 2023, **145**, 20655–20664.
171 Y. Xu, J. P. Edwards, S. Liu, R. K. Miao, J. E. Huang, C. M. Gabardo, C. P. O'Brien, J. Li, E. H. Sargent and D. Sinton, *ACS Energy Lett.*, 2021, **6**, 809–815.
172 H. S. Jeon, J. Timoshenko, C. Rettenmaier, A. Herzog, A. Yoon, S. W. Chee, S. Oener, U. Hejral, F. T. Haase and B. Roldan Cuenya, *J. Am. Chem. Soc.*, 2021, **143**, 7578–7587.
173 C. Kim, L.-C. Weng and A. T. Bell, *ACS Catal.*, 2020, **10**, 12403–12413.
174 H. Liu, T. Yan, S. Tan, L. Sun, Z. Zhang, S. Hu, S.-H. Li, X. Kang, Y. Lei, L. Jiang, T. Hou, L. Liu, Q. Yu and B. Liu, *J. Am. Chem. Soc.*, 2024, **146**, 5333–5342.
175 C. Kittel, *Introduction to solid state physics*, Wiley, Hoboken, NJ, 8th edn, 2005.
176 U. Mizutani, M. Inukai, H. Sato and E. S. Zijlstra, *Physical Metallurgy*, ed. D. E. Laughlin and K. Hono, Elsevier, Oxford, 2014, 5th edn, pp. 103–202, DOI: 10.1016/B978-0-444-53770-6.00002-2.
177 L. Xu and M. Mavrikakis, *J. Catal.*, 2024, **431**, 115373.
178 B. Hammer and J. K. Norskov, *Nature*, 1995, **376**, 238–240.
179 J. Kok, J. de Ruiter, W. van der Stam and T. Burdyny, *J. Am. Chem. Soc.*, 2024, **146**, 19509–19520.
180 J. B. Goodenough, *Chem. Mater.*, 2014, **26**, 820–829.
181 X. Zheng, B. Zhang, P. De Luna, Y. Liang, R. Comin, O. Voznyy, L. Han, F. P. García de Arquer, M. Liu, C. T. Dinh, T. Regier, J. J. Dynes, S. He, H. L. Xin, H. Peng, D. Prendergast, X. Du and E. H. Sargent, *Nat. Chem.*, 2018, **10**, 149–154.
182 F. Song, K. Schenk and X. Hu, *Energy Environ. Sci.*, 2016, **9**, 473–477.
183 L. Chong, G. Gao, J. Wen, H. Li, H. Xu, Z. Green, J. D. Sugar, A. J. Kropf, W. Xu, X.-M. Lin, H. Xu, L.-W. Wang and D.-J. Liu, *Science*, 2023, **380**, 609–616.
184 J. Huang, J. Chen, T. Yao, J. He, S. Jiang, Z. Sun, Q. Liu, W. Cheng, F. Hu, Y. Jiang, Z. Pan and S. Wei, *Angew. Chem., Int. Ed.*, 2015, **54**, 8722–8727.
185 Q. He, H. Xie, Z. U. Rehman, C. Wang, P. Wan, H. Jiang, W. Chu and L. Song, *ACS Energy Lett.*, 2018, **3**, 861–868.
186 R. Ram, L. Xia, H. Benzidi, A. Guha, V. Golovanova, A. Garzón Manjón, D. Llorens Rauret, P. Sanz Berman, M. Dimitropoulos, B. Mundet, E. Pastor, V. Celorrio, C. A. Mesa, A. M. Das, A. Pinilla-Sánchez, S. Giménez, J. Arbiol, N. López and F. P. García de Arquer, *Science*, 2024, **384**, 1373–1380.
187 B.-Q. Li, Z.-J. Xia, B. Zhang, C. Tang, H.-F. Wang and Q. Zhang, *Nat. Commun.*, 2017, **8**, 934.
188 S. Ye, Y. Lei, T. Xu, L. Zheng, Z. Chen, X. Yang, X. Ren, Y. Li, Q. Zhang and J. Liu, *Appl. Catal., B*, 2022, **304**, 120986.
189 R. Zhang, N. Dubouis, M. Ben Osman, W. Yin, M. T. Sougrati, D. A. D. Corte, D. Giaume and A. Grimaud, *Angew. Chem., Int. Ed.*, 2019, **58**, 4571–4575.
190 A. E. Thorarinsdottir, S. S. Veroneau and D. G. Nocera, *Nat. Commun.*, 2022, **13**, 1243.
191 M. R. Mohammadi, S. Loos, P. Chernev, C. Pasquini, I. Zaharieva, D. González-Flores, P. Kubella, K. Klingan, R. D. L. Smith and H. Dau, *ACS Catal.*, 2020, **10**, 7990–7999.
192 T. N. Nguyen, Z. Chen, A. S. Zeraati, H. S. Shiran, S. M. Sadaf, M. G. Kibria, E. H. Sargent and C.-T. Dinh, *J. Am. Chem. Soc.*, 2022, **144**, 13254–13265.
193 J. Wang, X. Jing, Y. Yang, B. Xu, R. Jia and C. Duan, *J. Am. Chem. Soc.*, 2024, **146**, 19951–19961.
194 M. W. Kanan and D. G. Nocera, *Science*, 2008, **321**, 1072–1075.
195 C. Feng, F. Wang, Z. Liu, M. Nakabayashi, Y. Xiao, Q. Zeng, J. Fu, Q. Wu, C. Cui, Y. Han, N. Shibata, K. Domen, I. D. Sharp and Y. Li, *Nat. Commun.*, 2021, **12**, 5980.
196 M. Chatti, J. L. Gardiner, M. Fournier, B. Johannessen, T. Williams, T. R. Gengenbach, N. Pai, C. Nguyen, D. R. MacFarlane, R. K. Hocking and A. N. Simonov, *Nat. Catal.*, 2019, **2**, 457–465.
197 W. Du, Y. Shi, W. Zhou, Y. Yu and B. Zhang, *Angew. Chem., Int. Ed.*, 2021, **60**, 7051–7055.
198 S. Cobo, J. Heidkamp, P.-A. Jacques, J. Fize, V. Fourmond, L. Guetaz, B. Jousselme, V. Ivanova, H. Dau, S. Palacin, M. Fontecave and V. Artero, *Nat. Mater.*, 2012, **11**, 802–807.
199 C. He, X. Wu and Z. He, *J. Phys. Chem. C*, 2014, **118**, 4578–4584.
200 Y. Wang, W. Zhou, R. Jia, Y. Yu and B. Zhang, *Angew. Chem., Int. Ed.*, 2020, **59**, 5350–5354.
201 L. Qiao, D. Liu, A. Zhu, J. Feng, P. Zhou, C. Liu, K. W. Ng and H. Pan, *Appl. Catal., B*, 2024, **340**, 123219.
202 S. Li, P. Ma, C. Gao, L. Liu, X. Wang, M. Shakouri, R. Chernikov, K. Wang, D. Liu, R. Ma and J. Wang, *Energy Environ. Sci.*, 2022, **15**, 3004–3014.
203 J. Zhang, T. Quast, B. Eid, Y.-T. Chen, R. Zerdoumi, S. Dieckhöfer, J. R. C. Junqueira, S. Seisel and W. Schuhmann, *Nat. Commun.*, 2024, **15**, 8583.
204 K. Wu, C. Sun, Z. Wang, Q. Song, X. Bai, X. Yu, Q. Li, Z. Wang, H. Zhang, J. Zhang, X. Tong, Y. Liang, A. Khosla and Z. Zhao, *ACS Mater. Lett.*, 2022, **4**, 650–656.
205 H. Jung, S. Y. Lee, C. W. Lee, M. K. Cho, D. H. Won, C. Kim, H.-S. Oh, B. K. Min and Y. J. Hwang, *J. Am. Chem. Soc.*, 2019, **141**, 4624–4633.
206 S. C. Lee, J. D. Benck, C. Tsai, J. Park, A. L. Koh, F. Abild-Pedersen, T. F. Jaramillo and R. Sinclair, *ACS Nano*, 2016, **10**, 624–632.
207 T. Ito, J. Raj, T. Zhang, S. Roy and J. Wu, *EES Catal.*, 2024, **2**, 997–1005.
208 A. T. Tabereaux and R. D. Peterson, *Treatise on Process Metallurgy*, ed. S. Seetharaman, R. Guthrie, A. McLean, S. Seetharaman and H. Y. Sohn, Elsevier, 2nd edn, 2024, pp. 625–676, DOI: 10.1016/B978-0-323-85373-6.00004-1.
209 U. DOE-OIT, *Prepared by Energetics Incorporated*, Columbia, Maryland, USA, 2000.
210 H. Ito and A. Manabe, in *Electrochemical Power Sources: Fundamentals, Systems, and Applications*, ed. T. Smolinka and J. Garche, Elsevier, 2022, pp. 281–304, DOI: 10.1016/B978-0-12-819424-9.00011-2.
211 S.-F. Zhao, M. Horne, A. M. Bond and J. Zhang, *J. Phys. Chem. C*, 2016, **120**, 23989–24001.
212 F. Li, Y. C. Li, Z. Wang, J. Li, D.-H. Nam, Y. Lum, M. Luo, X. Wang, A. Ozden and S.-F. Hung, *Nat. Catal.*, 2020, **3**, 75–82.
213 A. Guha, S. Narayanaru, N. M. Kaley, D. Krishna Rao, J. Mondal and T. N. Narayanan, *Mater. Today Commun.*, 2019, **21**, 100700.
214 J. Guo, Y. Zheng, Z. Hu, C. Zheng, J. Mao, K. Du, M. Jaroniec, S.-Z. Qiao and T. Ling, *Nat. Energy*, 2023, **8**, 264–272.
215 M. A. Khan, T. Al-Attas, S. Roy, M. M. Rahman, N. Ghaffour, V. Thangadurai, S. Larter, J. Hu, P. M. Ajayan and M. G. Kibria, *Energy Environ. Sci.*, 2021, **14**, 4831–4839.
216 L. Rebollar, S. Intikhab, N. J. Oliveira, Y. Yan, B. Xu, I. T. McCrum, J. D. Snyder and M. H. Tang, *ACS Catal.*, 2020, **10**, 14747–14762.
217 S. Paul, S. Sarkar, A. Adalder, A. Banerjee and U. K. Ghorai, *J. Mater. Chem. A*, 2023, **11**, 13249–13254.
218 J. Mukherjee, S. Paul, A. Adalder, S. Kapse, R. Thapa, S. Mandal, B. Ghorai, S. Sarkar and U. K. Ghorai, *Adv. Funct. Mater.*, 2022, **32**, 2200882.
219 L. Niu, L. An, X. Wang and Z. Sun, *J. Energy Chem.*, 2021, **61**, 304–318.
220 H. Cai, Z. Wang, G. Meng, T. Wei, Y. Liu, J. Luo, Q. Liu, G. Hu and X. Liu, *Inorg. Chem.*, 2024, **63**, 20935–20939.
221 Y. Xiong, Y. Wang, J. Zhou, F. Liu, F. Hao and Z. Fan, *Adv. Mater.*, 2024, **36**, 2304021.

